

# dMRI Distortion Correction: A Deep Learning-based Registration Approach

Zhangxing Bian and Zhiwei Gong

## Abstract

*Medical image registration is a fundamental task for various research and applications. Unfortunately, solving a pairwise optimization can be computationally intensive and therefore slow in practice. The non-deep learning based algorithms running on the CPU can require hours to register a pair of images, which becomes longer when registering 3D volumes. In this project, we explored the possibility of applying deep learning to 3D medical image registration, especially deformable registration. We focus on the application of correcting the distortion of diffusion MRI using a single phase-encoded B0 image and a T1w image through inter-modality registration. We novelly applied a differentiable Mutual Information loss to the task of dMRI distortion correction, and our model performs better than SyN and VoxelMorph over three metrics (CC, MI, SSIM).*

**Index Terms:** *deformable registration, convolutional neural networks, neuroimaging.*

## 1. Introduction

With diffusion magnetic resonance imaging (dMRI), it is possible to visualize and map the diffusion of water molecules in biological tissues in a non-invasive way [21, 34], as well as obtain valuable information about tissue microstructure [25] and the anatomical connections of the brain in a technique known as fiber tractography [24, 23, 40]. dMRIs have been acquired primarily using echo-planar imaging (EPI) [26], which allows a large number of diffusion-weighted images (DWIs) to be acquired in a short period of time. Nevertheless, geometric and intensity distortions of DWIs generated by susceptibility induced field defects (B0 field inhomogeneities) in combination with limited bandwidth in the phase-encode (PE) direction, generating spatial distortion along the PE axis, are an important issue with EPI [16, 2]. As a result, image analysis may be limited in affected regions, and alternative contrasts that provide structural information may be misaligned [14, 39].

It is generally necessary to modify the sequence (for example, parallel imaging, greater bandwidth) or acquire additional data to reduce or correct EPI distortions. The most commonly used techniques for correcting distortions are B0 mapping [16, 8, 35], estimation of point spread functions [42, 41], registration of distorted diffusion images using a non-rigid registration framework (a synthesized contrast

[28]) from distorted diffusion images (typically a T1- or T2-weighted contrast) [39, 20, 11, 33, 13]. Our work is registration-based and is most relevant to the last category.

The newly developed "blip-up blip-down" acquisitions [2] produce pairs of images with the same contrast but distortions reversed in directions. By warping the two images to their mid-point, the undistorted image will be obtained. However, it needs a reversed-gradient acquisition, which a lot of datasets do not have. Our model only requires a single gradient direction image to perform the correction.

Deformable registration-based correction is widely used for generating undistorted MRI. An image pair can be deformable registered using dense, non-linear correspondences. Traditional registration approaches involve aligning voxels with similar appearances while imposing constraints on the registration mapping in order to solve the optimization problem. However, to register a pair of scans with excellent precision, state-of-the-art algorithms operating on the CPU might take tens of minutes to hours [9, 18, 5]. Although recent GPU implementations have decreased the duration to minutes, each registration still requires a GPU [22].

The learning-based framework of VoxelMorph [6] formulates registration as a function that transforms a pair of input images into a deformation field that aligns them, and then uses a CNN to parameterize the function and uses a series of images to optimize the neural network's parameters. VoxelMorph quickly computes a deformation field given a fresh pair of scans by simply evaluating the function.

Based on VoxelMorph framework [6], the training strategy we use is unsupervised, the model is trained to optimize typical image matching objective functions. We achieve a comparable or even better performance to state-of-the-art registration while reducing the time by orders of magnitude. Registering takes less than a minute of CPU time and less than two seconds of GPU time, compared to dozens of minutes to more than two hours on the CPU for the most advanced non-deep learning baselines.

This report is organized as follows. **Section 2** will introduce some basic knowledge of deformable registration, then **Section 3** shows some related work. **Section 4** presents our methods. **Section 5** shows our experiments including the dataset we use, evaluation metrics, and experiments results. Implementation details, the insights of results and conclusion will be discussed in **Section 6**.

## 2. Background

For neuroimage registration, an initial affine transformation for global alignment is commonly followed by a considerably slower deformable transformation with additional degrees of freedom in deformable registration schemes. We focus on the last stage, which involves computing a dense, nonlinear correspondence for all voxels.

The majority of known deformable registration techniques use an energy function to repeatedly optimize a transformation [31]. Define  $f$  and  $m$  the fixed and moving image, respectively, and  $\phi$  as the registration field maps  $f$  to  $m$ . Then the optimization problem can be represented as the following:

$$\hat{\phi} = \arg \min_{\phi} \mathcal{L}(f, m, \phi) \quad (1)$$

$$= \arg \min_{\phi} \mathcal{L}_{sim}(f, m \circ \phi) + \lambda \mathcal{L}_{smooth}(\phi), \quad (2)$$

where  $\mathcal{L}_{sim}$  represents the similarity between two input images,  $\mathcal{L}_{smooth}$  defines the regularization,  $m \circ \phi$  denotes  $m$  wrapped by  $\phi$  and  $\lambda$  is the regularization trade-off parameter.

Intensity mean squared error, mutual information [38], and cross-correlation [4] are some of the most commonly used metrics for  $\mathcal{L}_{sim}$ . When volumes have different intensity distributions and contrasts, the last two are particularly beneficial.  $\mathcal{L}_{smooth}$  imposes a spatially smooth deformation, which is frequently described as a function of a displacement vector field's ( $\mathbf{u}$ ) spatial gradients. For each volume pair, traditional techniques optimize Eq.1. When registering a large number of volumes, this is costly. In contrast, we substitute pair-specific deformation field optimization with global optimization of the common parameters, which is known as amortization in other areas [17, 30]. After estimating the global function, a deformation field may be generated by evaluating the function on a specific volume pair.

## 3. Related work

### 3.1. FSL TOPUP

As part of the FSL software package [15, 29], TOPUP which is renamed based on the technique developed by Andersson et al. [3] has been incorporated into their preprocessing pipeline for dMRI images, becoming a widely used blip-up blip-down correction method, as well as the tool of choice for the Human Connectome project [32]. This acquisition is typical to acquire data using reverse-phase encoding directions, which results in varying degrees and orientations of distortion, supporting the estimation of an undistorted volume. However, not all imaging protocols enable a blip-up blip-down or equivalent acquisition, therefore TOPUP's advanced susceptibility and motion correction features are unavailable. For instance, a vast majority of datasets of the past have not been collected with

this modification, and this modification may be difficult to adopt in research and clinical setting. Moreover, many clinically deployed software releases do not support blip-up blip-down acquisitions. For that purpose, a distortion correction algorithm is needed such that it works with widely available diffusion imaging data, associated clinically common sequences like anatomical structural MRI data with diffusion imaging data with a *single* PE direction.

### 3.2. Traditional Registration (Non-learning-based)

Image registration is an essential step for many medical imaging tasks, such as atlas-based segmentation, atlas generation, and surveillance of tumor growth. Among all the algorithms that have been developed, diffeomorphic transforms [4, 37] have shown great success in various computational anatomy studies. However, these approaches optimize an energy function for given image pair, resulting in slow registration, ranging from tens of minutes to hours. Long registration time impedes large-scale atlas reconstruction and group analysis.

### 3.3. Deep Learning-based Registration

In order to solve the aforementioned problem, a number of recent articles have proposed that neural networks be used to train a function for medical image registration. The majority of these rely on ground truth warp fields [7, 19], which may be produced by simulating deformations and distorted pictures or by using traditional registration algorithms to pairs of scans. Image similarity is also used by some to assist with registration [7]. While supervised approaches are promising, ground truth warp fields obtained from traditional registration tools as ground truth can be time-consuming to obtain and limit the types of deformations that can be learnt. The unsupervised VoxelMorph [6] learns a parameterized registration function, which takes two 3D input volumes and outputs a mapping of all voxels of one volume to another volume. It achieves comparable accuracy to the best traditional registration while taking less than a minute using a CPU and under a second on a GPU. However, for inter-modality registration, VoxelMorph relies on Cross-correlation similarity measurement that is sensitive to the choice of window size and usually suffers from large anatomical differences. In this work, we built our model based on VoxelMorph, but adopted a differentiable mutual information loss and applied it to our distortion correction task with a few modifications that are proved to be beneficial.

## 4. Method

We denote  $f, m$  as two image volumes over a 3-D spatial domain  $\Omega \subset \mathbb{R}^3$ .  $g_\theta(f, m) = \mathbf{u}$  is the function that we model by the CNN, where  $\theta$  are the kernels of the convolutional layers.

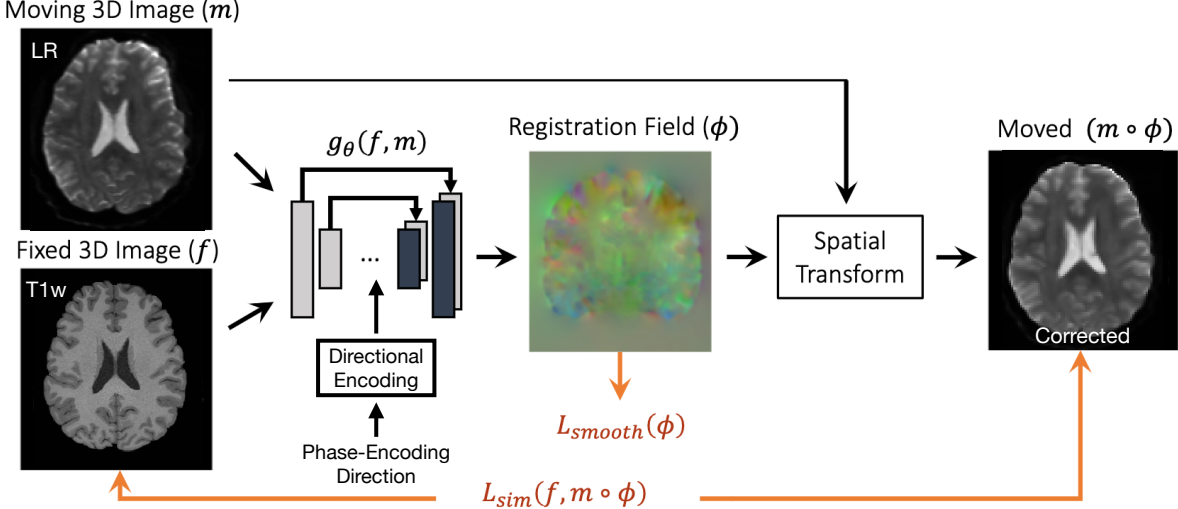


Figure 1. The framework of our method. Given a fixed image, which is distortion-free, and a b0 image from the diffusion MRI, which suffers from geometric distortion, the Unet-like network predicts the deformation that corrects the distortion. Phase-encoding is mapped through the Directional Encoding layer to an embedding vector, which is injected into the decoder to help predict the deformation field. (This figure is modified from VoxelMorph.)

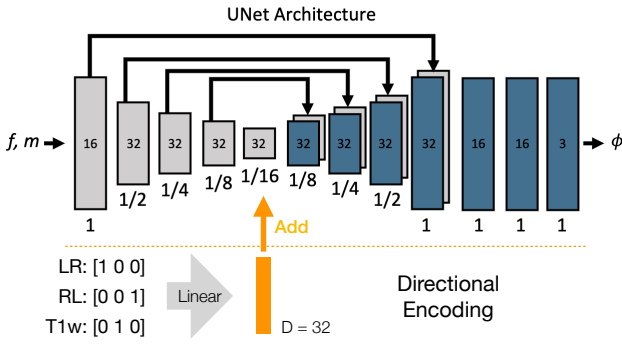


Figure 2. Our Directional Encoding module. We use the same Unet backbone as VoxelMorph. Exceptionally, we map the phase-encoding directions to an embedding vector through a linear layer and add it to the beginning of the decoder.

Fig.1 shows the framework of our method. We take  $f$  and  $m$  as input of the network, and then use  $g_\theta$  to get  $\phi$ . The phase-encoding direction is projected by a linear layer to a embedding vector, which is added to the deepest features of the Unet as shown in Fig. 2.  $m$  is warped to  $m \circ \phi$  by the spatial transformation function. Given a new pair of images  $f$  and  $m$  in test time, the corresponding deformation field will be obtained by evaluating  $g_\theta(f, m)$ .

#### 4.1. Spatial Transformation Function

Since we aim to minimize the disparities between  $m \circ \phi$  and  $f$ , standard gradient-based method is performed. We use the same spatial transformation function as VoxelMorph

[6] to compute  $m \circ \phi$ :

$$m \circ \phi(\mathbf{p}) = \sum_{\mathbf{q} \in \mathcal{Z}(\mathbf{p}')} m(\mathbf{q}) \prod_{d \in \{x, y, z\}} (1 - |\mathbf{p}'_d - \mathbf{q}_d|), \quad (3)$$

where  $\mathbf{p}' = \mathbf{p} + \mathbf{u}(\mathbf{p})$  is a subpixel voxel location in  $m$  for the corresponding voxel  $\mathbf{p}$ ,  $d$  iterates over dimensions of  $\Omega$  and  $\mathcal{Z}(\mathbf{p}')$  are the voxel neighbors of  $\mathbf{p}'$ .

#### 4.2. Loss Functions

**Cross-correlation Loss** As in VoxelMorph [6], we use the local cross-correlation between the two images  $f$  and  $m \circ \phi$  (as one of our baselines):

$$CC(f, m \circ \phi) = \quad (4)$$

$$\sum_{\mathbf{p} \in \Omega} \frac{\left( \sum_{\mathbf{p}_i} (f(\mathbf{p}_i) - \hat{f}(\mathbf{p}))([m \circ \phi](\mathbf{p}_i) - [\hat{m} \circ \phi](\mathbf{p}_i)) \right)^2}{\left( \sum_{\mathbf{p}_i} (f(\mathbf{p}_i) - \hat{f}(\mathbf{p}))^2 \right) \left( \sum_{\mathbf{p}_i} ([m \circ \phi](\mathbf{p}_i) - [\hat{m} \circ \phi](\mathbf{p}_i))^2 \right)}, \quad (5)$$

where  $\hat{f}(\mathbf{p}) = \frac{1}{n^3} \sum_{\mathbf{p}_i} f(\mathbf{p}_i)$  and  $[\hat{m} \circ \phi](\mathbf{p})$  represent local mean intensity images,  $\mathbf{p}_i$  iterates over a  $n^3$  volume around  $\mathbf{p}$ , in our experiment, we use  $n = 9$ .

To use the CC-based loss function, we define the similarity loss as following:

$$\mathcal{L}_{sim}(f, m, \phi) = -CC(f, m \circ \phi), \quad (6)$$

where a higher value of CC presents a better alignment. We referred Eq.6 as negative cross-correlation loss (NCC) in the following section.

**Smoothness Loss** The regularization term  $\mathcal{L}_{smooth}(\phi)$  is defined as:

$$\mathcal{L}_{smooth}(\phi) = \sum_{\mathbf{p} \in \Omega} \|\nabla \mathbf{u}(\mathbf{p})\|^2. \quad (7)$$

**Differentiable Mutual Information Loss** Since we aim to perform inter-modality registration between T1w and B0 images that have different intensities, we adopted the information-based similarity measurement — mutual information, which has been widely used in multi-modal registration [27].

The mutual information between two images A and B is originally defined as the following:

$$I(A, B) = \sum_{a,b} p(a, b) \log \frac{p(a, b)}{p(a)p(b)}. \quad (8)$$

The probability  $p(a)$  is the percentage of the voxels in image A with intensity a, and the probability  $p(b)$  is likewise for image B. And  $p(a, b)$  is the joint distribution of the intensities of two images A and B. To practically implement this, one needs to bin intensities to calculate Eq. 8 in a discrete manner, which is not differentiable.

To solve this problem, Parzen windowing [27] can be used to calculate the continuous contribution of each voxel to a range of histogram bins, instead of contributing only to the bin it falls into [10].

Thus, we calculate  $P(x)$  as follows: given a set of  $n$  samples  $S$ , each sample's contribution is weighted by a Gaussian function of its distance to  $x$ :

$$P_S(x) = \frac{1}{n} \sum_{s \in S} W(x - s), \quad (9)$$

where function  $W$ , with a parameter  $\sigma$  is defined as:

$$W(x - s) = \frac{1}{\sigma \sqrt{2\pi}} e^{-\frac{(x-s)^2}{2\sigma^2}} \quad (10)$$

The intensity distribution of a single image A is given by  $P_A(x)$ , and likewise  $P_B(x)$  for image B. The joint probability can be calculated as:

$$P_{A,B}(x, y) = \frac{1}{n} \sum_{(a,b) \in (A, B)} W(x - a)W(y - b) \quad (11)$$

To use this MI-based loss function, we define the similarity loss as following:

$$\mathcal{L}_{sim}(A, B) = -I(A, B) \quad (12)$$

## 5. Experiments

### 5.1. Experimental Setup

#### 5.1.1 Dataset

Training a DL-based registration model *from scratch* requires a large dataset and computational resources. For example, VoxelMorph trained their network on 3231 brain MRI scans, each scan of size 160x192x224. The authors find with 100 training images, VoxelMorph leads to state-of-the-art registration quality. In our work, due to the limit of time and computational resources, we plan to take the pre-trained model and finetune it for our task.

We worked on HCP [36] and Buckner40 dataset [9]. HCP [36] is a large public available brain MR dataset that contains 1200 subjects' 3T MR imaging data. It has several MR modalities imaging for each subject, such as diffusion MR and structural MR (T1w and T2w), which can be used as material for different modality registration. We randomly extract 102 subjects as a subset for us to work with. Buckner40 dataset [9] contains manual annotations for 30 structures. We used this dataset to show qualitatively how our method performs on the intra-modality registration.

#### 5.1.2 Evaluation Metrics

It is usually impossible to obtain the ground truth of the deformation field since different registration fields can yield similar-looking warped images. So measure the registration performance by:

(1) Qualitative visual checking. Visually check several main structures to see if they are well aligned, e.g., cortical grey matter and ventricles.

(2) Since T1 and b0 are two different modalities, L1 and L2 will not be reasonable similarity measurements. Thus, we quantitatively measure the similarity through SSIM, Cross-correlation, and Mutual Information, which are not sensitive to the absolute difference in image intensity.

#### 5.1.3 Implementation Details

We set the weight of smoothness penalty to 1.0 for training with NCC loss and 0.1 for training with MI loss. The weight setting for NCC loss is the same as VoxelMorph, and the weight for MI loss is empirically determined.

We adopted the same training strategy for training VoxelMorph baseline and our model. We use early stopping with three epochs tolerance. Adam with Cyclic lr scheduler [1e-4, 5e-4] is used as the optimizer. We use batchsize 1 due to the limit of GPU RAM. The training curve is shown in Fig.5. For testing, both methods run fast (less than 2s) on 1070Ti. The framework is implemented in Pytorch.

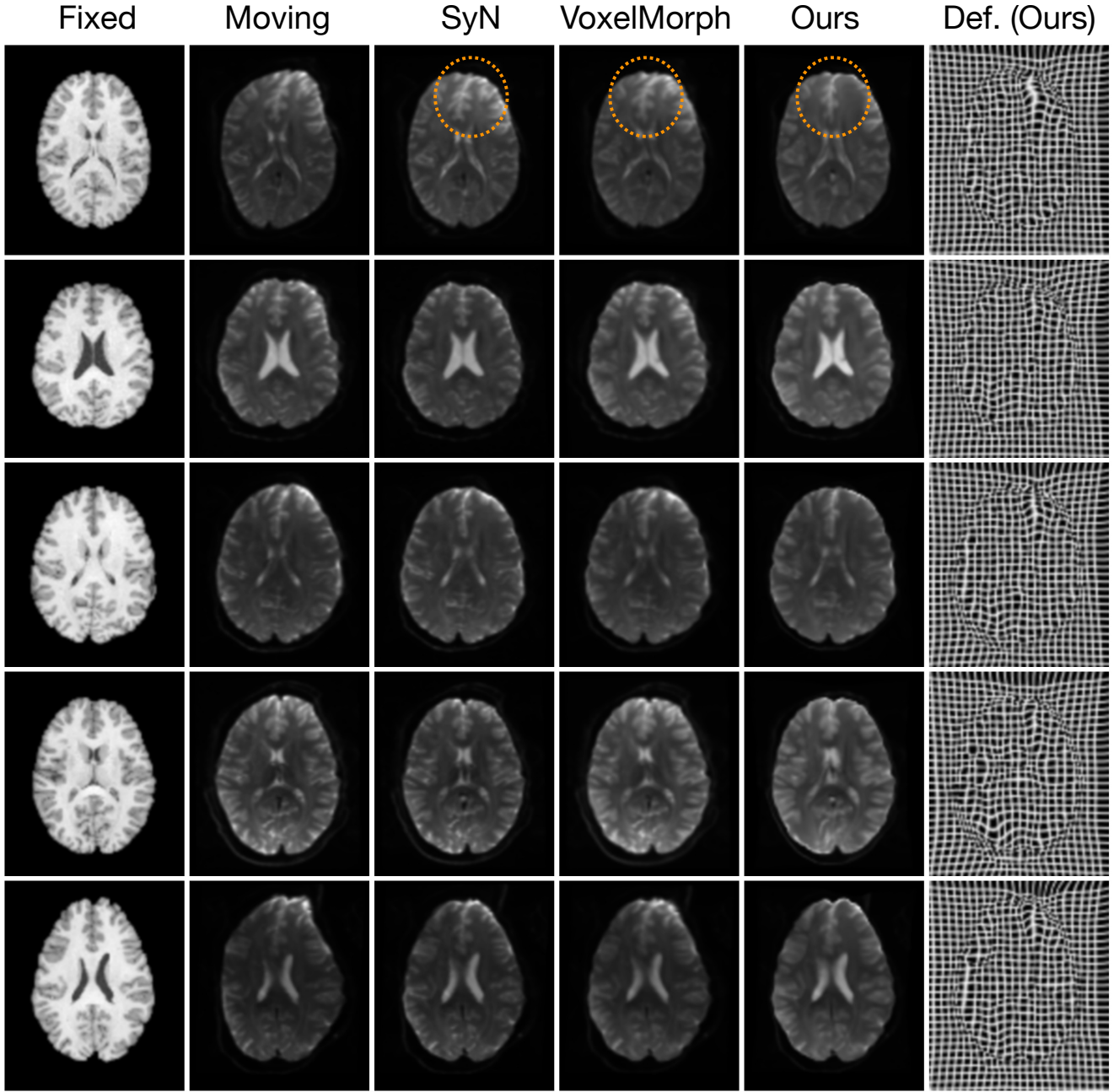


Figure 3. Qualitative comparison. The first two columns represent the T1 image (fixed) and b0 image (moving). The following three columns represent the correction results (warped moving) of three methods: SyN, VoxelMorph, and ours. The frontal lobe (which is circled in the first row) is most susceptible to distortion corruption. The deformation field is shown in the last column. None of the subjects is seen during the training.

## 5.2. Distortion Correction

We apply our model to correct the distortion of diffusion MRI with an undistorted T1w image. For each subject, we extract B0 images from the diffusion-weighted image sequence and the averaged image as one of the inputs (mov-

ing image) to our model. We use the corresponding T1w image as the fixed image. The model predicts the deformation field, which is used to warp the moving image to a fixed image, i.e., correct the distortion of the diffusion MR image (B0).

We tested our model and two other baselines on the held-

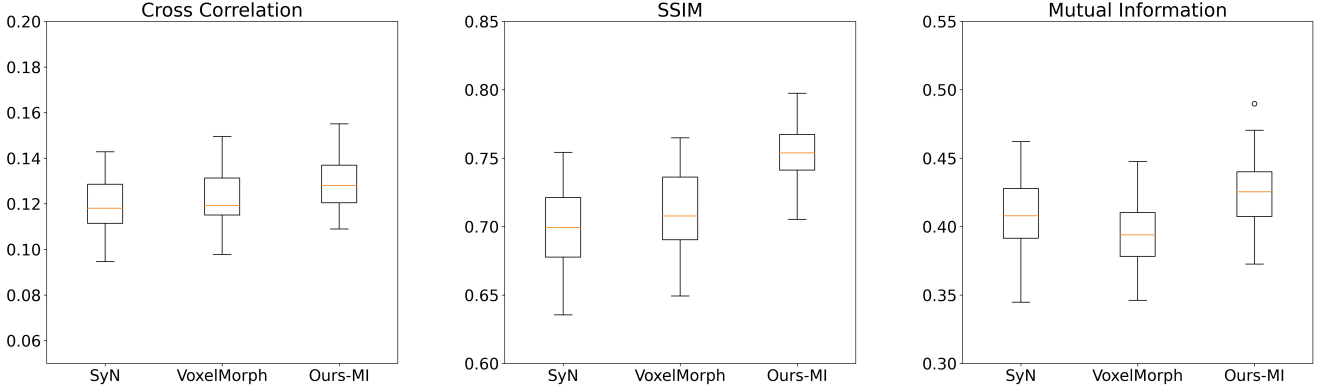


Figure 4. Quantitative comparison. We measure the similarity between fixed image and warped moving image through three metrics: SSIM↑, Cross-correlation↑, and Mutual Information↑. 31 different subjects from test set are evaluated. ↑ indicates the higher is better.



Figure 5. Training process. The training loss and validation loss are plotted against gradient descent steps.

out test set, which was not seen during the training. As Fig.3 shows, our method performs correction visually better than the other two baselines, especially in the most susceptible region – the frontal lobe. We also compare three methods quantitatively on three metrics: SSIM, Cross-correlation, and Mutual Information, as shown in Fig.4. Our model performs consistently better than the other two baselines on all metrics. Interestingly, SyN method, despite its slowness, performs better than VoxelMorph in terms of Mutual Information.

### 5.3. Subject-to-Subject Registration

Besides diffusion MRI distortion correction, which focuses on inter-modality registration, we also applied our model to register different subjects, which could serve as a powerful tool for applications such as multi-atlas segmentation [1, 12].

We used differentiable MI loss to train the model, and the pairs of T1 images for training were randomly sampled from the train split of Buckner dataset on the fly. During testing, the resulting deformation field is used to warp the atlas segmentations through nearest-neighbor interpolation. A few qualitative results are shown in the Fig.6.

## 6. Discussion and Conclusion

We frame the problem of correcting distortion of diffusion MRI as a registration problem. Inspired by VoxelMorph, we adopted a differentiable mutual information loss and directional embedding module to perform the inter-modality registration task. We achieved better performance than SyN and VoxelMorph. We also explore the possibility of applying our model to perform subject to subject registration (intra-modality task).

Despite the preliminary success in correcting geometric distortion using our approach, the non-uniform magnetic field will also cause a loss of signal, which cannot be recovered by registration only. Recovering signal loss and correcting geometric distortion *at the same time* could be a promising future direction.

## References

- [1] P. Aljabar, R. A. Heckemann, A. Hammers, J. V. Hajnal, and D. Rueckert. Multi-atlas based segmentation of brain images: atlas selection and its effect on accuracy. *Neuroimage*, 46(3):726–738, 2009.
- [2] J. Andersson and S. Skare. Image distortion and its correction in diffusion mri. *Diffusion MRI: Theory, Methods, and Applications*. Oxford University Press, Oxford, pages 285–302, 2010.
- [3] J. L. Andersson, S. Skare, and J. Ashburner. How to correct susceptibility distortions in spin-echo echo-planar images: application to diffusion tensor imaging. *Neuroimage*, 20(2):870–888, 2003.
- [4] B. B. Avants, C. L. Epstein, M. Grossman, and J. C. Gee. Symmetric diffeomorphic image registration with cross-correlation: evaluating automated labeling of elderly and neurodegenerative brain. *Medical image analysis*, 12(1):26–41, 2008.
- [5] B. B. Avants, N. J. Tustison, G. Song, P. A. Cook, A. Klein, and J. C. Gee. A reproducible evaluation of ants similarity

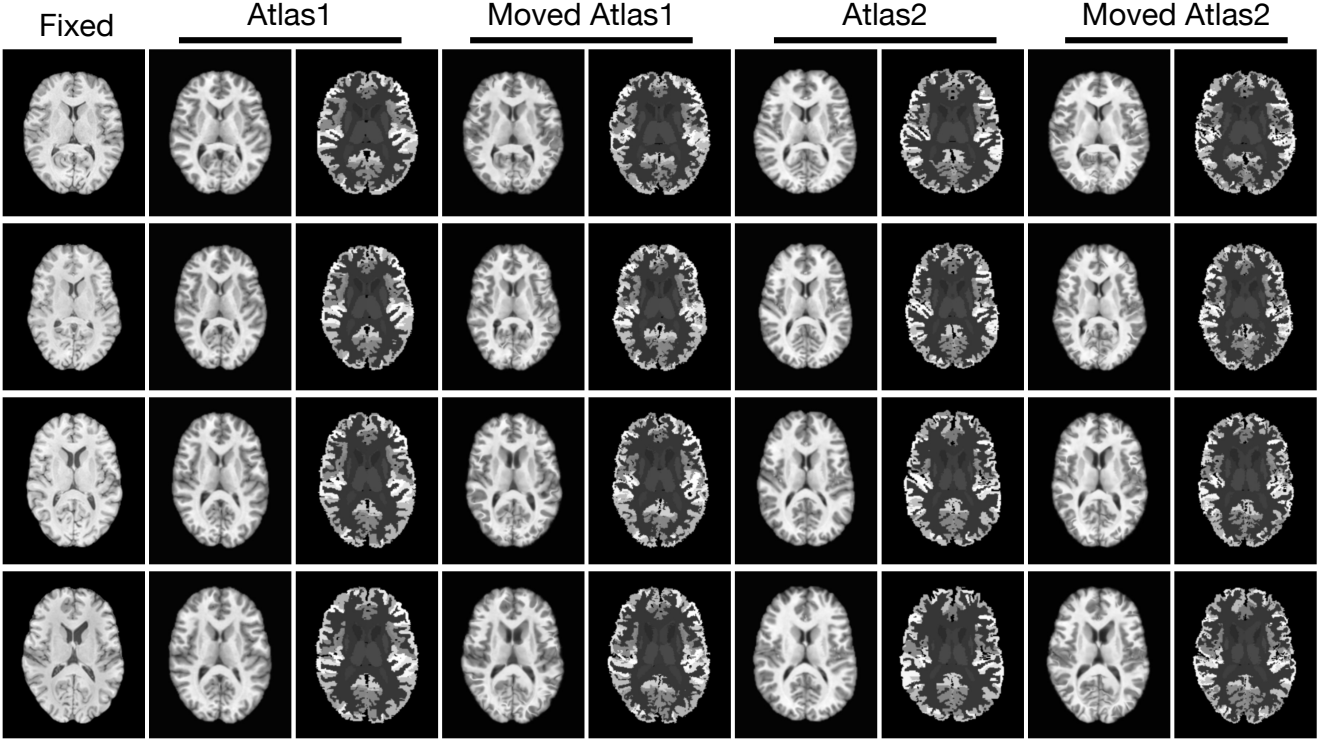


Figure 6. Qualitative results of subject-to-subject registration. For each row, one fixed image, two atlas images, and registration results are shown. Each atlas consists of a T1 image and a manually labeled segmentation. Note that the subjects of fixed and atlases images are different, thus the anatomical structure can be very dissimilar.

- metric performance in brain image registration. *Neuroimage*, 54(3):2033–2044, 2011.
- [6] G. Balakrishnan, A. Zhao, M. R. Sabuncu, J. Guttag, and A. V. Dalca. Voxelmorph: a learning framework for deformable medical image registration. *IEEE transactions on medical imaging*, 38(8):1788–1800, 2019.
  - [7] X. Cao, J. Yang, J. Zhang, D. Nie, M. Kim, Q. Wang, and D. Shen. Deformable image registration based on similarity-steered cnn regression. In *International Conference on Medical Image Computing and Computer-Assisted Intervention*, pages 300–308. Springer, 2017.
  - [8] N.-k. Chen and A. M. Wyrwicz. Correction for epi distortions using multi-echo gradient-echo imaging. *Magnetic Resonance in Medicine: An Official Journal of the International Society for Magnetic Resonance in Medicine*, 41(6):1206–1213, 1999.
  - [9] B. Fischl. Freesurfer. *Neuroimage*, 62(2):774–781, 2012.
  - [10] C. K. Guo. *Multi-modal image registration with unsupervised deep learning*. PhD thesis, Massachusetts Institute of Technology, 2019.
  - [11] H. Huang, C. Ceritoglu, X. Li, A. Qiu, M. I. Miller, P. C. van Zijl, and S. Mori. Correction of b0 susceptibility induced distortion in diffusion-weighted images using large-deformation diffeomorphic metric mapping. *Magnetic resonance imaging*, 26(9):1294–1302, 2008.
  - [12] J. E. Iglesias and M. R. Sabuncu. Multi-atlas segmentation of biomedical images: a survey. *Medical image analysis*, 24(1):205–219, 2015.
  - [13] M. O. Irfanoglu, L. Walker, S. Sammet, C. Pierpaoli, and R. Machiraju. Susceptibility distortion correction for echo planar images with non-uniform b-spline grid sampling: a diffusion tensor image study. In *International Conference on Medical Image Computing and Computer-Assisted Intervention*, pages 174–181. Springer, 2011.
  - [14] M. O. Irfanoglu, L. Walker, J. Sarlls, S. Marenco, and C. Pierpaoli. Effects of image distortions originating from susceptibility variations and concomitant fields on diffusion mri tractography results. *Neuroimage*, 61(1):275–288, 2012.
  - [15] M. Jenkinson, C. F. Beckmann, T. E. Behrens, M. W. Woolrich, and S. M. Smith. Fsl. *Neuroimage*, 62(2):782–790, 2012.
  - [16] P. Jezzard and R. S. Balaban. Correction for geometric distortion in echo planar images from b0 field variations. *Magnetic resonance in medicine*, 34(1):65–73, 1995.
  - [17] Y. Kim, S. Wiseman, A. Miller, D. Sontag, and A. Rush. Semi-amortized variational autoencoders. In *International Conference on Machine Learning*, pages 2678–2687. PMLR, 2018.
  - [18] A. Klein, J. Andersson, B. A. Ardekani, J. Ashburner, B. Avants, M.-C. Chiang, G. E. Christensen, D. L. Collins, J. Gee, P. Hellier, et al. Evaluation of 14 nonlinear defor-

- mation algorithms applied to human brain mri registration. *Neuroimage*, 46(3):786–802, 2009.
- [19] J. Krebs, T. Mansi, H. Delingette, L. Zhang, F. C. Ghesu, S. Miao, A. K. Maier, N. Ayache, R. Liao, and A. Kammen. Robust non-rigid registration through agent-based action learning. In *International Conference on Medical Image Computing and Computer-Assisted Intervention*, pages 344–352. Springer, 2017.
- [20] J. Kybic, P. Thévenaz, A. Niriko, and M. Unser. Unwarping of unidirectionally distorted epi images. *IEEE transactions on medical imaging*, 19(2):80–93, 2000.
- [21] D. Le Bihan, E. Breton, D. Lallemand, P. Grenier, E. Cabanis, and M. Laval-Jeantet. Mr imaging of intravoxel incoherent motions: application to diffusion and perfusion in neurologic disorders. *Radiology*, 161(2):401–407, 1986.
- [22] M. Modat, G. R. Ridgway, Z. A. Taylor, M. Lehmann, J. Barnes, D. J. Hawkes, N. C. Fox, and S. Ourselin. Fast free-form deformation using graphics processing units. *Computer methods and programs in biomedicine*, 98(3):278–284, 2010.
- [23] S. Mori, B. J. Crain, V. P. Chacko, and P. C. Van Zijl. Three-dimensional tracking of axonal projections in the brain by magnetic resonance imaging. *Annals of Neurology: Official Journal of the American Neurological Association and the Child Neurology Society*, 45(2):265–269, 1999.
- [24] S. Mori and P. C. Van Zijl. Fiber tracking: principles and strategies—a technical review. *NMR in Biomedicine: An International Journal Devoted to the Development and Application of Magnetic Resonance In Vivo*, 15(7-8):468–480, 2002.
- [25] D. S. Novikov, E. Fieremans, S. N. Jespersen, and V. G. Kiselev. Quantifying brain microstructure with diffusion mri: Theory and parameter estimation. *NMR in Biomedicine*, 32(4):e3998, 2019.
- [26] R. Ordidge. The development of echo-planar imaging (epi): 1977–1982. *Magnetic Resonance Materials in Physics, Biology and Medicine*, 9(3):117–121, 1999.
- [27] J. P. Pluim, J. A. Maintz, and M. A. Viergever. Mutual-information-based registration of medical images: a survey. *IEEE transactions on medical imaging*, 22(8):986–1004, 2003.
- [28] S. Roy, Y.-Y. Chou, A. Jog, J. A. Butman, and D. L. Pham. Patch based synthesis of whole head mr images: Application to epi distortion correction. In *International Workshop on Simulation and Synthesis in Medical Imaging*, pages 146–156. Springer, 2016.
- [29] S. M. Smith, M. Jenkinson, M. W. Woolrich, C. F. Beckmann, T. E. Behrens, H. Johansen-Berg, P. R. Bannister, M. De Luca, I. Dronjak, D. E. Flitney, et al. Advances in functional and structural mr image analysis and implementation as fsl. *Neuroimage*, 23:S208–S219, 2004.
- [30] C. K. Sønderby, J. Caballero, L. Theis, W. Shi, and F. Huszár. Amortised map inference for image super-resolution. *arXiv preprint arXiv:1610.04490*, 2016.
- [31] A. Sotiras, C. Davatzikos, and N. Paragios. Deformable medical image registration: A survey. *IEEE transactions on medical imaging*, 32(7):1153–1190, 2013.
- [32] S. N. Sotiropoulos, S. Jbabdi, J. Xu, J. L. Andersson, S. Moeller, E. J. Auerbach, M. F. Glasser, M. Hernandez, G. Sapiro, M. Jenkinson, et al. Advances in diffusion mri acquisition and processing in the human connectome project. *Neuroimage*, 80:125–143, 2013.
- [33] R. Tao, P. T. Fletcher, S. Gerber, and R. T. Whitaker. A variational image-based approach to the correction of susceptibility artifacts in the alignment of diffusion weighted and structural mri. In *International Conference on Information Processing in Medical Imaging*, pages 664–675. Springer, 2009.
- [34] D. Taylor and M. Bushell. The spatial mapping of translational diffusion coefficients by the nmr imaging technique. *Physics in medicine & biology*, 30(4):345, 1985.
- [35] U. Techavipoo, A. F. Okai, J. Lackey, J. Shi, M. A. Dresner, T. P. Leist, and S. Lai. Toward a practical protocol for human optic nerve dti with epi geometric distortion correction. *Journal of Magnetic Resonance Imaging: An Official Journal of the International Society for Magnetic Resonance in Medicine*, 30(4):699–707, 2009.
- [36] D. C. Van Essen, S. M. Smith, D. M. Barch, T. E. Behrens, E. Yacoub, K. Ugurbil, W.-M. H. Consortium, et al. The wu-minn human connectome project: an overview. *Neuroimage*, 80:62–79, 2013.
- [37] T. Vercauteren, X. Pennec, A. Perchant, and N. Ayache. Diffeomorphic demons: Efficient non-parametric image registration. *NeuroImage*, 45(1):S61–S72, 2009.
- [38] P. Viola and W. M. Wells III. Alignment by maximization of mutual information. *International journal of computer vision*, 24(2):137–154, 1997.
- [39] M. Wu, L.-C. Chang, L. Walker, H. Lemaitre, A. S. Barnett, S. Marenco, and C. Pierpaoli. Comparison of epi distortion correction methods in diffusion tensor mri using a novel framework. In *International Conference on Medical Image Computing and Computer-Assisted Intervention*, pages 321–329. Springer, 2008.
- [40] R. Xue, P. C. Van Zijl, B. J. Crain, M. Solaiyappan, and S. Mori. In vivo three-dimensional reconstruction of rat brain axonal projections by diffusion tensor imaging. *Magnetic Resonance in Medicine: An Official Journal of the International Society for Magnetic Resonance in Medicine*, 42(6):1123–1127, 1999.
- [41] M. Zaitsev, J. Hennig, and O. Speck. Point spread function mapping with parallel imaging techniques and high acceleration factors: Fast, robust, and flexible method for echo-planar imaging distortion correction. *Magnetic Resonance in Medicine: An Official Journal of the International Society for Magnetic Resonance in Medicine*, 52(5):1156–1166, 2004.
- [42] H. Zeng and R. T. Constable. Image distortion correction in epi: comparison of field mapping with point spread function mapping. *Magnetic Resonance in Medicine: An Official Journal of the International Society for Magnetic Resonance in Medicine*, 48(1):137–146, 2002.